

# Herpes simplex virus type 1 thymidine kinase–armed bovine herpesvirus type 4–based vector displays enhanced oncolytic properties in immunocompetent orthotopic syngenic mouse and rat glioma models

Marco Redaelli, Valentina Franceschi, Antonio Capocéfalo, Domenico D'Avella, Luca Denaro, Sandro Cavirani, Carla Mucignat-Caretta, and Gaetano Donofrio

*Department of Human Anatomy and Physiology, University of Padova, Padova, Italy (M.R., C.M.-C.); Department of Animal Health, University of Parma, Parma, Italy (V.F., A.C., S.C., G.D.); Department of Neuroscience, University of Padova, Padova, Italy (D.D., L.D.)*

Gliomas are devastating tumors of the brain resistant to therapies. Although some therapies can prolong the survival time among the affected persons, gliomas are not curable and new therapeutic approaches need to be investigated. Oncolytic viruses seem to represent an interesting alternative, because anticancer agents and new viral agents have to be explored to identify the one with the best characteristics. Bovine herpesvirus type 4 (BoHV-4) is a gammaherpesvirus with a striking tropism and permissive replication toward cancer cells and rat, mouse, and human glioma cells. However, BoHV-4 does not replicate into the normal brain parenchyma. The BoHV-4 genome was cloned as a bacterial artificial chromosome to easily manipulate this large genome and be used as a viral vector platform. In the present study, a herpes simplex virus type 1 thymidine kinase suicide gene–armed BoHV-4 was constructed, characterized, and proven to be highly efficient in killing by apoptosis glioma cells *in vitro* when co-administered with the pro-drug ganciclovir (GCV). When the armed BoHV-4/GCV therapeutic approach was tested in immunocompetent orthotopic syngenic mouse and rat glioma models *in vivo*, a significant increase in survival among the treated animals was achieved, and some animals were

completely cured. The BoHV-4–based vector represents a promising alternative oncolytic virus for glioma and, perhaps, other types of cancer treatment that merit further investigation. This article represents the result of a mutual interaction between human medical science and veterinary science, a combination of scientific knowledge often neglected.

**Keywords:** bovine herpesvirus, gliomas, oncolytic virus, orthotopic, syngenic model.

**G**liomas are glia-derived neoplasms of the brain. According to the classification of the World Health Organization (WHO), the grades 3 and 4 are also known as malignant gliomas. The grade 3 gliomas include the anaplastic astrocytoma and anaplastic oligodendroglioma, whereas the grade 4 is represented by the glioblastoma multiforme (GBM).<sup>1</sup> These gliomas are characterized by highly replicating and rarely metastatic tumor cells with a variety of acquired genetic alterations that confer them resistance to therapy.<sup>2</sup> Median survival time among patients with a malignant glioma has remained essentially the same in the past 3 decades and is generally agreed to be 18–20 months for the anaplastic astrocytoma and 8–14 months for GBM.<sup>3,4</sup> Surgery, radiotherapy, and chemotherapy, used alone or in combination, are the current standard therapies of early diagnosed malignant gliomas.<sup>2</sup> Although treatments may prolong survival and improve quality of life, there are no curative treatments for malignant gliomas. For this reason, new therapeutic approaches, even if only experimental, have been

Received August 2, 2011; accepted November 15, 2011.

**Corresponding Author:** Gaetano Donofrio, DVM, PhD, Dipartimento di Salute Animale, Sezione di Malattie Infettive degli Animali, Università di Parma, via del Taglio 8-43126 Parma, Italy (gaetano.donofrio@unipr.it).

generated to improve the outcome of these devastating tumors.

Replication-competent oncolytic viruses, either naturally occurring or genetically engineered, represent a new class of anticancer agents being developed and tested in the clinical and preclinical setting. These agents, with their capacity to amplify their dose through replication at the target site, spread within the tumor to lyse neoplastic cells and decrease the tumor burden, representing unique anticancer therapeutics.<sup>5</sup> It is difficult to predict from the current knowledge of various potential viral agents which virus could best fulfill the oncolytic goals. Consequently, new oncolytic agents based on viruses must be investigated.

Bovine herpesvirus type 4 (BoHV-4) is a gamma-herpesvirus belonging to the genus *Rhadinovirus*. BoHV-4 has been isolated from a variety of samples and cells from healthy cattle and from cattle that have experienced abortion or have metritis, pneumonia, diarrhea, respiratory infection, and/or mammary pustular dermatitis.<sup>6</sup> However, the pathogenic role of BoHV-4 remains unclear, and only a few investigators have successfully produced experimental disease.<sup>6</sup> The virus was first isolated in Europe from cattle with respiratory and ocular diseases by Bartha et al.<sup>7</sup> and later in the United States by Mohanty et al.<sup>8</sup> Subsequently, distinct BoHV-4 isolates were obtained both in Europe and in the United States.<sup>9–11</sup> Although BoHV-4 is classified as a gammaherpesvirus based on genome sequencing,<sup>12</sup> it differs from other gammaherpesvirus members in important biological properties: little or no pathogenicity, no oncogenicity, efficiently replicates and causes cytopathic effect (CPE) in a variety of primary cultures and cell lines of various animal species,<sup>13</sup> and has a striking tropism toward many human cancer cells.<sup>14,15</sup> Furthermore, BoHV-4 has the ability to accommodate large amounts of foreign genetic material within its genome without any appreciable detrimental effect on its replication. For these reasons, it has been proposed as a viral vector for gene delivery and cancer therapy.<sup>16</sup> To better exploit such characteristics, a nonpathogenic strain of BoHV-4 was isolated from the cell milk fraction of a healthy cow, and its genome was cloned as a bacterial artificial chromosome (BAC) to be better genetically manipulated and used as a vector platform.<sup>17</sup>

BoHV-4 does not replicate in mouse or rat brain, but reporter gene expression has been shown in ependymal cells and the rostral migratory stream area after injection into the lateral ventricle of both mouse and rat brain.<sup>18,19</sup> Furthermore, BoHV-4 replication was observed when intramurally injected into experimentally generated rat brain tumour.<sup>20</sup> These results prompted us to use BoHV-4 as a vector for gene therapy or oncolytic therapy of brain tumors. In the present article, the oncolytic properties of a new recombinant herpes simplex virus type 1 thymidine kinase (HSV-1-TK)-armed BoHV-4 have been investigated.

## Materials and Methods

### Cells

Madin Derby Bovine Kidney (MDBK; ATCC, CCL-22), bovine embryo kidney (BEK; from Dr. M. Ferrari), BEK-expressing cre recombinase (BEK<sup>cre</sup>),<sup>17</sup> human rhabdomyosarcoma (RD-4; from Dr. V. van Santen), human embryo kidney 293T (HEK 293T; ATCC, CRL-11268), mouse glioblastoma (GL261; obtained from the National Cancer Institute), rat glioma ((F98; ATCC, CRL-2397), and human glioma (GLI36; a gift from Dr. A. Campagni) cell lines were cultured in Dulbecco's modified essential medium (DMEM; Sigma) containing 10% fetal bovine serum (FBS), 2 mM of L-glutamine, 100 IU/mL of penicillin (Sigma), 100 µg/mL of streptomycin (Sigma), and 2.5 µg/mL of amphotericin B. Primary bovine endometrial stromal cells were obtained from Dr. M. Sheldon and kept in RPMI-1640 (Sigma) containing 10% FBS, 50 IU/mL penicillin, 50 µg/mL streptomycin, and 2.5 µg/mL amphotericin B.

The primary human cell culture (P26)<sup>20</sup> was prepared from a glioblastoma biopsy sample (patient, 70-year-old man). The biopsy sample (3 mm<sup>3</sup>) was shaken for 5 min in 3 mL of 0.25% Trypsin, 0.02% EDTA solution. The suspension was inactivated with growth media (DMEM) containing 10% FBS, 2 mM of L-glutamine, 100 IU/mL of penicillin, 100 µg/mL of streptomycin, and 2.5 µg/mL of amphotericin B and centrifuged at 1350 rpm for 10 min at 37°C. The supernatant was discharged, and the pellet was resuspended in 10 mL of growth media and plated in a cell culture flask. The culture was monitored for 3 weeks, changing the medium every 3 days and maintained as described above for 60 passages before freezing. The tests were performed after thawing on the fourth passage.

### Plasmids

The 1.2-kb fragment containing the entire HSV-1-TK open reading frame (ORF) was excised from the pHyTK plasmid vector (kindly provided by Dr. Cornel Fraefel) with *NheI*/*PmeI* restriction enzymes and subcloned in pIRES2DsRED-Express2 vector (Clontech) linearized with *NheI*/*SmaI* to generate the pCMVie-TK<sup>HSV-1</sup>-IRES-dsRed-pA vector. Next, the TK<sup>HSV-1</sup>-IRES-dsRed module was excised with *NheI*/*NotI* restriction enzymes and subcloned in the pINT2GFP vector<sup>16</sup> cut with *NheI*/*SmaI* and, thus, deprived of the GFP ORF. Thus, the pTK-hCMVie-TK<sup>HSV-1</sup>-IRES-dsRed-pA-TK construct was obtained. All the restriction and DNA modifying enzymes were purchased from Fermentas.

### Transient Transfection Assay

Confluent HEK293T cells in 6-well plates were transfected with pCMVie-TK<sup>HSV-1</sup>-IRES-dsRed-pA or pTK-hCMVie-TK<sup>HSV-1</sup>-IRES-dsRed-pA-TK, using LTX

transfection reagent (Invitrogen) as suggested by the manufacturer. The transfection mixture was prepared in DMEM/high glucose without serum and antibiotics and left on the cells for 6 h at 37°C, 5% CO<sub>2</sub>, in a humidified incubator. After 6 h, the transfection mixture was replaced with complete medium (EMEM, 10% FBS, 50 IU/mL penicillin, 50 µg/mL streptomycin, and 2.5 µg/mL amphotericin B) and left to recover for 18 h at 37°C, 5% CO<sub>2</sub> in air, in a humidified incubator. At 24 h after transfection, cells were extracted to be analyzed by Western immunoblotting.

#### *BAC BoHV-4 Recombineering and Selection*

Recombineering was performed as previously described<sup>17</sup> and<sup>21</sup> with some modifications. SW102 bacteria containing KanaGalK targeted into the BoHV-4-A thymidine kinase<sup>17</sup> locus were grown, heat-induced, and electroporated with a gel-purified fragment (TK-hCMVie-TK<sup>HSV-1</sup>-IRES-dsRed-pA-TK) obtained by cutting pTK-hCMVie-TK<sup>HSV-1</sup>-IRES-dsRed-pA-TK with XhoI/ClaI. After electroporation for the counterselection step, the bacteria were recovered in 10 mL LB in a 50-mL baffled conical flask and incubated for 4.5 h in a 32°C shaking water bath. Bacterial serial dilutions were plated on M63 minimal medium plates containing 15 g/L agar, 0.2% glycerol (Sigma), 1 mg/L D-biotin, 45 mg/L L-leucine, 0.2% 2-deoxygalactose (Sigma), and 25 µg/mL chloramphenicol. Plates were incubated for 3–5 days at 32°C. Several selected colonies were picked up, streaked on MacConkey agar indicator plates (Difco; BD Biosciences) containing 20 µg/mL of chloramphenicol, and incubated at 32°C for 3 days until white colonies appeared. White colonies were grown in duplicate for 5–8 h in 1 mL of LB containing 50 µg/mL of kanamycin or LB containing 20 µg/mL of chloramphenicol. Only those colonies growing on chloramphenicol and not on kanamycin were kept and grown overnight in 5 mL of LB containing 20 µg/mL of chloramphenicol. BAC-BoHV-4-A was purified and analyzed through HindIII restriction enzyme digestion for TK-hCMVie-TK<sup>HSV-1</sup>-IRES-dsRed-pA-TK fragment targeted integration.

Original detailed protocols for recombineering can also be found at the recombineering Web site (<http://recombineering.ncifcrf.gov>).

#### *Recombinant BAC-BoHV-4 Genome Characterization*

pBAC-BoHV-4-A and pBAC-BoHV-4-A-hCMVie-TK<sup>HSV-1</sup>-IRES-dsRed-pA were characterized using 50 µL of DNA prepared from 5 mL of SW102 bacteria containing BACs, HindIII restriction enzyme digested, separated by electrophoresis overnight in a 1% agarose gel, stained with ethidium bromide, capillary transferred to a positively charged nylon membrane (Roche), and cross-linked by UV irradiation by standard procedures. The membrane was prehybridized in 50 mL of hybridization solution (7% sodium dodecyl sulfate, 0.5 M phosphate, pH 7.2, 1 mM EDTA) for 2 h at 65°C in a

rotating hybridization oven (Techna Instruments). Probe preparation and digoxigenin nonisotopic labeling were performed by polymerase chain reaction (PCR). Five microliters of the probe were added to 100 µL of double-distilled water in a screw-cap tube, denatured in boiling water for 5 min, and cooled on ice for another 2 min. The denatured probe was added to the hybridization solution, and the membrane was hybridized overnight at 65°C in a rotating hybridization oven (Techna Instruments). Following hybridization, the membrane was washed and blocked in 25 mL of blocking solution. Antidigoxigenin Fab fragment (150 U/200 µL; Roche), diluted 1:15 000 in 25 mL of blocking solution, was applied to the membrane, and detection was performed following equilibration of the membrane in detection buffer for 2 min at room temperature. Chemiluminescent substrate (Roche) was added by scattering the drops over the surface of the membrane. After placement of the membrane between 2 plastic sheets, any bubbles present under the sheet were eliminated with a damp laboratory tissue to create a liquid seal around the membrane. Signal detection was obtained by exposing the membrane to X-ray film. The exposure time was adjusted with the intensity of the signal.

#### *Cell Culture Electroporation and Recombinant Virus Reconstitution*

pBAC-BoHV-4-A or pBAC-BoHV-4-A-hCMVie-TK<sup>HSV-1</sup>-IRES-dsRed-pA plasmid DNA (5 µg) in 500 µL DMEM without serum was electroporated (Equibio apparatus; 270 V, 960 µF, 4-mm-gap cuvettes) into BEK or BEK<sup>cre</sup> cells from a confluent 25-cm<sup>2</sup> flask. Electroporated cells were returned to the flask, fed the next day, and split 1:2 when they reached confluence at 2 days postelectroporation. Cells were left to grow until CPE appeared. Recombinant viruses were propagated by infecting confluent monolayers of MDBK cells at an MOI of 0.5 TCID<sub>50</sub> per cell and maintaining them in MEM with 10% FBS for 2 h. The medium was then removed and replaced with fresh MEM containing 10% FBS. When ~90% of the cell monolayer exhibited CPE (~72 h postinfection), the virus was prepared by freezing and thawing cells 3 times and pelleting virions through 30% sucrose, as described previously.<sup>18</sup> Virus pellets were resuspended in cold MEM without FBS. TCID<sub>50</sub> was determined on MDBK cells by limiting dilution.

#### *Viral Growth Curves and Plaque Assay*

BEK cells were infected with BoHV-4-A and BoHV-4-A-hCMVie-TK<sup>HSV-1</sup>-IRES-dsRed-pA at an MOI of 1 TCID<sub>50</sub>/cell and incubated at 37°C for 4 h. Infected cells were washed with serum-free EMEM and then overlaid with EMEM containing 10% FBS, 2 mM L-glutamine, 100 IU/mL penicillin (Sigma), 100 µg/mL streptomycin (Sigma), and 2.5-µg/mL amphotericin B. The supernatants of infected cultures

were harvested after 12, 24, 36, 48, 60, and 72 h, and the amount of infectious virus was determined by limiting dilution on BEK cells. For the plaque assays, Vero cell monolayers were infected with serial 10-fold dilutions of the respective viruses and overlaid with medium containing 1.5% methylcellulose at 2 h after infection. At 5 days postinfection, plaques were fixed with 10% formalin, stained with 0.5% crystal violet, and their size was estimated.

#### Western Immunoblotting

Cell extracts containing 50  $\mu$ g of total protein were electrophoresed through 10% sodium dodecyl sulfate-polyacrylamide gels and transferred to nylon membranes by electroblotting. Membranes were incubated with monoclonal anti-HSV-1 TK (clone sc-28037 [vN-20]; Santa Cruz Biotechnology), probed with horseradish peroxidase-labeled anti-mouse immunoglobulin antibody (Sigma), and visualized by enhanced chemiluminescence (ECL kit; Pierce).

#### Apoptotic/Necrotic Assay

GL261, F98, GLI36, and P26 cells were plated on 24-well plates and grown on 9-mm round sterile cover slips. After 24 h, cells were infected with BoHV-4-A, BoHV-4-A-hCMVie-TK<sup>HSV-1</sup>-IRES-dsRed, or PBS as control. The medium was renewed 72 h postinfection, and GCV (50  $\mu$ g/mL or PBS as control) was added for 72 h with a 6-group scheme: BoHV-4-A-hCMVie-TK<sup>HSV-1</sup>-IRES-dsRed, GCV, BoHV-4-A-hCMVie-TK<sup>HSV-1</sup>-IRES-dsRed + GCV, BoHV-4a, and BoHV-4-A + GCV. Cells were incubated for 24 h and then fixed with methanol and stained with Wright's stain; a total of 2400 cells were counted from each slide. The percentage of apoptotic and necrotic cells was then calculated, according to an established procedure;<sup>22</sup> *t* test was used to estimate the amount of apoptotic and necrotic cells (in percentage) between the groups.

#### In vivo – Healthy Mice

A preliminary in vivo screen was performed on healthy mice. Forty-eight 4-month-old male CD1 mice were pre-anesthetized with isoflurane and subsequently anesthetized with zolazepam tiletamine (20 mg/kg body weight) and xylazine (75 mg/kg body weight).

Twenty-four mice were inoculated with 2  $\mu$ L ( $2 \times 10^6$  pfu) BoHV-4<sup>TK<sup>HSV-1</sup></sup> and 24 with 2  $\mu$ L PBS into the left lateral ventricle of the brain (ICV), by a Hamilton syringe (0.5  $\mu$ L/min) using the stereotaxic coordinates from Bregma (AP + 1.5, ML – 1.0, DV – 2.0 mm). Three days after surgery, GCV (50 mg/kg body weight each dose) was administered with an intraperitoneal (ip) injection for 6 days to 12 BoHV-4-A-hCMVie-TK<sup>HSV-1</sup>-IRES-dsRed mice and to 12 PBS mice.

#### In vivo – Animal Glioma Models

Two animal models were created: the GL261/C57BL6J mouse glioblastoma and the F98/Fisher rat glioma model. Animals (60 C57BL6J mice and 60 Fisher rats) were pre-anesthetized with isoflurane and subsequently anesthetized with zolazepam tiletamine (20 mg/kg body weight) and xylazine (75 mg/kg body weight). All the animals were inoculated with syngenic cells ( $2 \times 10^6$  GL261 cells in 2  $\mu$ L and  $8 \times 10^6$  F98 cells in 8  $\mu$ L) using the stereotaxic coordinates from Bregma (AP + 1.5, ML – 1.0, DV – 2.0 mm for mice and AP + 1.0, ML – 1.5, DV – 3.7 mm for rats). Animals were monitored for 18 days postinfection, and only the animals that showed clinical evidence of a growing tumor mass from day 19 through day 22 were included in the experiment and randomly assigned to 1 of the 4 experimental groups. All of the in vivo experiments were performed according to the 116/92 Italian law on animal experiments and were approved by the local Ethical Committee.

## Results

#### Design and Expression of HSV-1-TK in a Bicistronic Expression Cassette and Construction of a Recombinant BoHV-4

BoHV-4 spontaneously exerts oncolytic effects with absence of infectivity or detrimental effect in the brain parenchyma when intracranially injected into experimentally generated rat brain tumors.<sup>20</sup> To further improve these oncolytic properties, it was thought to arm BoHV-4 with a suicide gene, such as HSV-1-TK. Therefore, the first concern was the generation of a suitable expression cassette to be integrated into the BoHV-4 genome to efficiently express an HSV-1-TK ORF. Enhancement of human cytomegalovirus immediate early promoter (hCMVie) activity was previously observed in cells infected with BoHV-4;<sup>17</sup> thus, the hCMVie promoter was chosen here to drive the expression of the HSV-1-TK ORF. Therefore, a bicistronic expression cassette (hCMVie-TK<sup>HSV-1</sup>-IRES-dsRed-pA) containing the hCMVie promoter followed by the HSV-1-TK ORF, an internal ribosomal entry site (IRES), the red fluorescent protein (RFP) ORF, and a polyadenylation signal (pA) was constructed (Fig. 1A). This bicistronic expression cassette allowed the detection of viral infection by fluorescence microscopy without the addition of antibodies or enzyme substrates. When HEK293T cells were transiently transfected with phCMVie-TK<sup>HSV-1</sup>-IRES-dsRed-pA, they abundantly expressed both proteins. The RFP (Fig. 1B) was detected by fluorescence microscopy, and HSV-1-TK (Fig. 1C) was detected by Western immunoblotting with an antibody against HSV-1-TK.

Although BoHV-4 possesses a TK gene and expresses a TK enzyme, BoHV-4 TK does not phosphorylate the pro-drug GCV.<sup>23</sup> To substitute BoHV-4 TK with HSV-1-TK, the hCMVie-TK<sup>HSV-1</sup>-IRES-

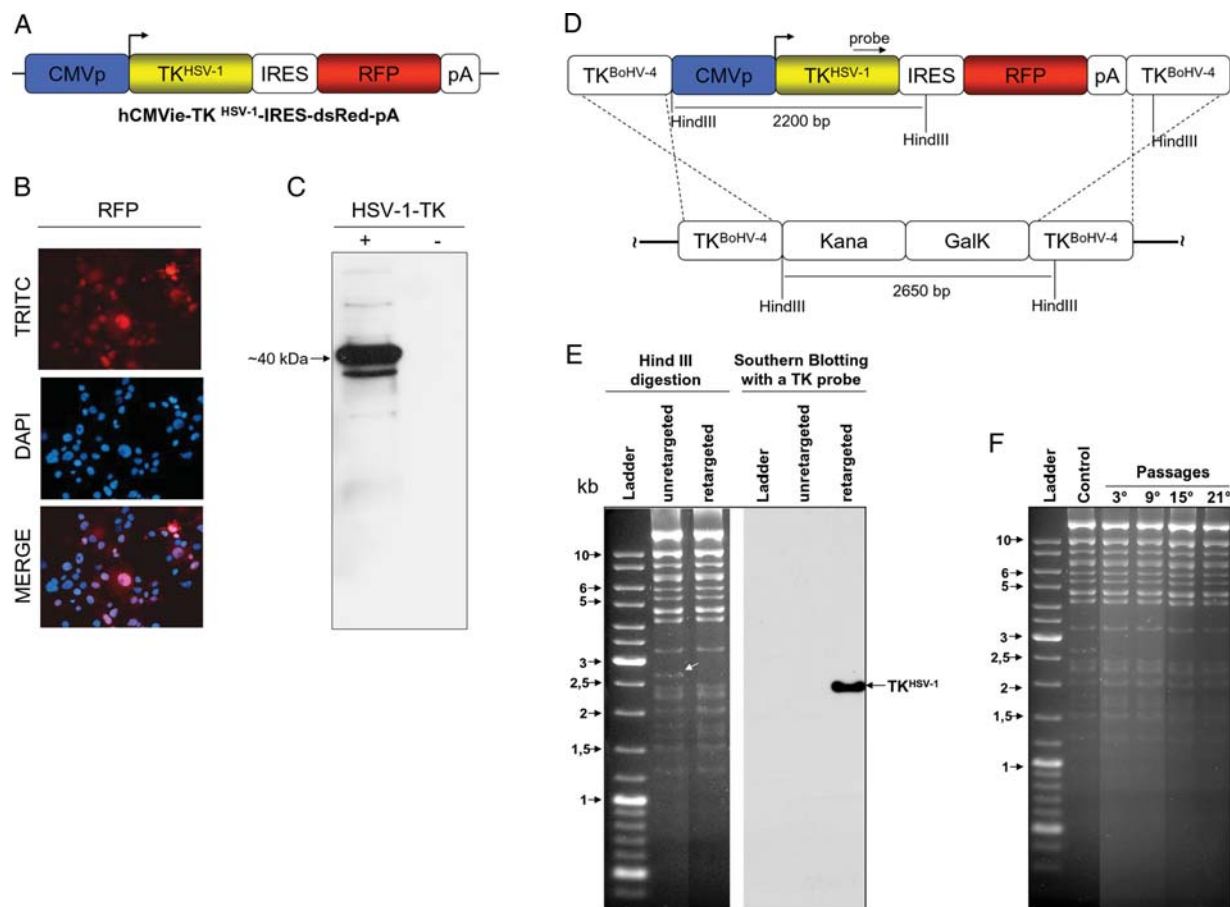


Fig. 1. A, hCMVie-TK<sup>HSV-1</sup>-IRES-dsRed-pA expression cassette diagram (not on scale) containing the human cytomegalovirus immediate early promoter (CMVp; blue), the HSV-1 -TK ORF (TK<sup>HSV-1</sup>; yellow), an internal ribosomal entry site (IRES; white), the red fluorescent protein ORF (RFP; red) and a polyadenylation signal (pA; white). B, Representative image of cells transiently transfected with hCMVie-TK<sup>HSV-1</sup>-IRES-dsRed-pA, expressing the RFP as visualized by a fluorescence microscope with a red filter (TRITC) and their nuclei counterstained with DAPI, which co-localized with red cells when overimposed (MERGE). C, Western immunoblotting of the same hCMVie-TK<sup>HSV-1</sup>-IRES-dsRed-pA transiently transfected cells expressing HSV-1-TK (+). A negative control was performed with cells transiently transfected with an empty vector (-). D, Schematic diagram (not on scale) of the retargeting strategy employed on BAC-BoHV-4-A genome targeted at the TK locus with a KanaGalk selectable cassette (pBAC-BoHV-4-A-TK-KanaGalk-TK). The Kana/Galk cassettes were removed via heat-inducible homologous recombination and replaced with hCMVie-TK<sup>HSV-1</sup>-IRES-dsRed-pA expression cassette. E, The selected colonies were tested through HindIII restriction enzyme analysis, agar gel electrophoresis and Southern blotting. The retargeted clones were detected through the disappearance of the 2.6 kb band (indicated by a white arrow) and the appearance of a 2.2 kb band detected by Southern blotting. F, pBAC-BoHV-4-A-hCMVie-TK<sup>HSV-1</sup>-IRES-dsRed-pA clonal stability in *Escherichia coli* SW102 cells, passaged for 21 consecutive days and analyzed by HindIII digestion and agarose gel electrophoresis. The untargeted pBAC-BoHV-4-A-TK-KanaGalk-TK was used as a control.

dsRed-pA expression cassette was inserted into the BAC-BoHV-4 TK genomic locus through heat-inducible homologous recombination.<sup>17</sup> hCMVie-TK<sup>HSV-1</sup>-IRES-dsRed-pA was first subcloned in pINT2,<sup>16</sup> a shuttle vector containing 2 BoHV-4 TK flanking regions, to obtain TK-hCMVie-TK<sup>HSV-1</sup>-IRES-dsRed-pA-TK and then shuttled in SW102 *Escherichia coli* containing the BAC-BoHV-4-A genome targeted at the TK locus with a KanaGalk selectable cassette<sup>17</sup> (Fig. 1D). The selected clones were first analyzed by PCR (data not shown), then by HindIII restriction profiling and Southern blotting with a specific probe for

HSV-1-TK (Fig. 1E). *E. coli* SW102 carrying heat-inducible recombinases after repeated passages could lead to a bacterial phenotype with a leaking transcription of the recombinases, even at temperatures that do not induce growth. Therefore, SW102 carrying pBAC-hCMVie-TK<sup>HSV-1</sup>-IRES-dsRed-pA was serially cultured over 20 passages. The pBAC-BoHV-4-A-hCMVie-TK<sup>HSV-1</sup>-IRES-dsRed-pA was then isolated and analyzed by HindIII restriction enzyme digestion, showing that no differences among restriction profiles at various periods of culture were observed (Fig. 1F).

### *HSV-1-TK Does Not Interfere with BoHV-4-A-TK<sup>HSV-1</sup>-IRES-dsRed Growth Characteristics*

Although the removal or interruption of the endogenous TK gene from the BoHV-4 genome did not lead to a detectable impairment of the viral phenotype,<sup>21</sup> it was of interest to know whether its substitution with a heterologous TK, such as HSV-1-TK, could have any effect. When pBAC-BoHV-4-A-hCMVie-TK<sup>HSV-1</sup>-IRES-dsRed-pA was electroporated into BEK or BEK<sup>cre</sup> cells, infectious viable virus was obtained in both cases (Fig. 2A). No differences in terms of the time needed to reconstitute the virus following cell electroporation were observed if compared with the parental pBAC-BoHV-4-A (3 days for both viruses) (Fig. 2B). Because BoHV-4 TK substitution with HSV-1-TK could have an impact on viral growth kinetics or plaque size, it was of interest to compare the growth characteristics of BoHV-4-A-hCMVie-TK<sup>HSV-1</sup>-IRES-dsRed with BoHV-4-A. BoHV-4-A-hCMVie-TK<sup>HSV-1</sup>-IRES-dsRed showed the same growth characteristics of the parental BoHV-4-A both in terms of growth kinetics (Fig. 2C) and plaque morphology and size (Fig. 2D and E).

### *BoHV-4-A-TK<sup>HSV-1</sup>-IRES-dsRed-infected Cells Express both RFP and HSV-1-TK and Are Responsive to GCV Treatment*

To verify the BoHV-4-A-TK<sup>HSV-1</sup>-IRES-dsRed transgene expression, cell lines and primary cell cultures were infected with BoHV-4-A-TK<sup>HSV-1</sup>-IRES-dsRed. The spread of infection was monitored at 24, 48, and 72 h postinfection by fluorescence microscopy and Western immunoblotting. All BoHV-4-A-TK<sup>HSV-1</sup>-IRES-dsRed-infected cell lines and primary cell cultures tested expressed both RFP and HSV-1-TK (Fig. 3 and Table 1 in supplementary File 1).

Next, the functionality of HSV-1-TK integrated into BoHV-4-A-TK<sup>HSV-1</sup>-IRES-dsRed was assessed on the RD-4 cell line. RD-4 cells were used because they are susceptible to BoHV-4 infection but resistant to CPE<sup>24</sup> induced by BoHV-4 replication. Therefore, it was possible to ascribe the cell death only to the GCV treatment and not to BoHV-4 infection. In fact, a strong CPE was only observed in BoHV-4-A-TK<sup>HSV-1</sup>-IRES-dsRed-infected and GCV-treated RD-4 cells. This effect was not observed in BoHV-4-A-infected RD-4 cells, either treated or untreated with GCV (Fig. 4A and B). Furthermore, a barely detectable difference of RD-4 cell growth was noticed when cells were treated with GCV (Fig. 4A and B). The cell death observed in BoHV-4-A-TK<sup>HSV-1</sup>-IRES-dsRed-infected and GCV-treated RD-4 cells was by apoptosis (Fig. 4C).

### *Oncolytic Properties of BoHV-4-A-TK<sup>HSV-1</sup>-IRES-dsRed/GCV on Glioma Cells In Vitro*

BoHV-4 induces CPE in glioma cells.<sup>20</sup> Therefore, before testing BoHV-4-A-hCMVie-TK<sup>HSV-1</sup>-IRES-

dsRed combined with GCV treatment in vivo, we tested the functionality of this combined treatment in vitro on a panel of mouse (GL261), rat (F98), and human (GLI36 and P26) glioma cells. Cells were infected with BoHV-4-A-hCMVie-TK<sup>HSV-1</sup>-IRES-dsRed or BoHV-4-A, treated or untreated with GCV, and then necrosis and apoptosis was measured (Fig. 5). A striking increase in apoptotic cell death was observed in cells infected with BoHV-4-A-hCMVie-TK<sup>HSV-1</sup>-IRES-dsRed and treated with GCV, compared with the controls (*t* test, *P* < .001) (Fig. 5A, C, E, G). The induced necrosis was significantly higher in the combined treatment group than in the others, in both the GL261 and F98 cells but not in GLI36 and P26 cells (*t* test, *P* < .001) (Fig. 6 B and D). In the human cells tested, the necrosis induced by the combined treatment was significantly lower if compared with the other BoHV-4 groups and significantly higher if compared with the GCV and control groups (*t* test, *P* < .001) (Fig. 6F and H). However, when apoptosis and necrosis were added together, 100% of cell death was observed in all cell types treated with BoHV-4-A-hCMVie-TK<sup>HSV-1</sup>-IRES-dsRed and GCV.

### *Oncolytic Properties of BoHV-4-A-TK<sup>HSV-1</sup>-IRES-dsRed/GCV in Immunocompetent Rat and Mouse Glioma Model In Vivo*

Notwithstanding the encouraging results obtained in vitro, before applying the same treatment regimen (BoHV-4-A-hCMVie-TK<sup>HSV-1</sup>-IRES-dsRed/GCV) in immunocompetent rat and mouse glioma models in vivo, the potential intrinsic toxicity of such treatment was tested first in healthy mice. The mice were intracerebrally inoculated with BoHV-4-A-hCMVie-TK<sup>HSV-1</sup>-IRES-dsRed and 6 days later intraperitoneally injected with GCV (*n* = 12) for 6 consecutive days (Fig. 6A). During the 90 days of observation, mice did not show any neurological symptoms or progressive loss of body weight, similarly to the 3 control groups (*n* = 12 each) (Fig. 6B).

Next, orthotopically grafted syngenic gliomas were generated in mice (*n* = 48, representing the 80% of GL261 cell-injected animals) and rats (*n* = 40, representing 66.7% of F98-injected animals). Animals were monitored after cell injection (Fig. 7A). Only the animals that showed clinical signs of the growing tumor mass from day 19 through day 22 were included in the experiment and randomly assigned to 1 of the 4 experimental groups: BoHV-4-A-hCMVie-TK<sup>HSV-1</sup>-IRES-dsRed + PBS (ICV BoHV-4-A-hCMVie-TK<sup>HSV-1</sup>-IRES-dsRed injection and IP PBS 6 days pi, for 6 days), PBS + GCV (ICV PBS injection and ip GCV 50 mg/kg body weight 6 days pi, for 6 days), BoHV-4-A-hCMVie-TK<sup>HSV-1</sup>-IRES-dsRed + GCV (ICV BoHV-4-A-hCMVie-TK<sup>HSV-1</sup>-IRES-dsRed injection and ip GCV 50 mg/kg body weight 6 days pi, for 6 days), and PBS + PBS (ICV PBS injection and ip PBS 6 days pi, for 6 days). Animals were monitored every day to determine variation in body and degree of neurological

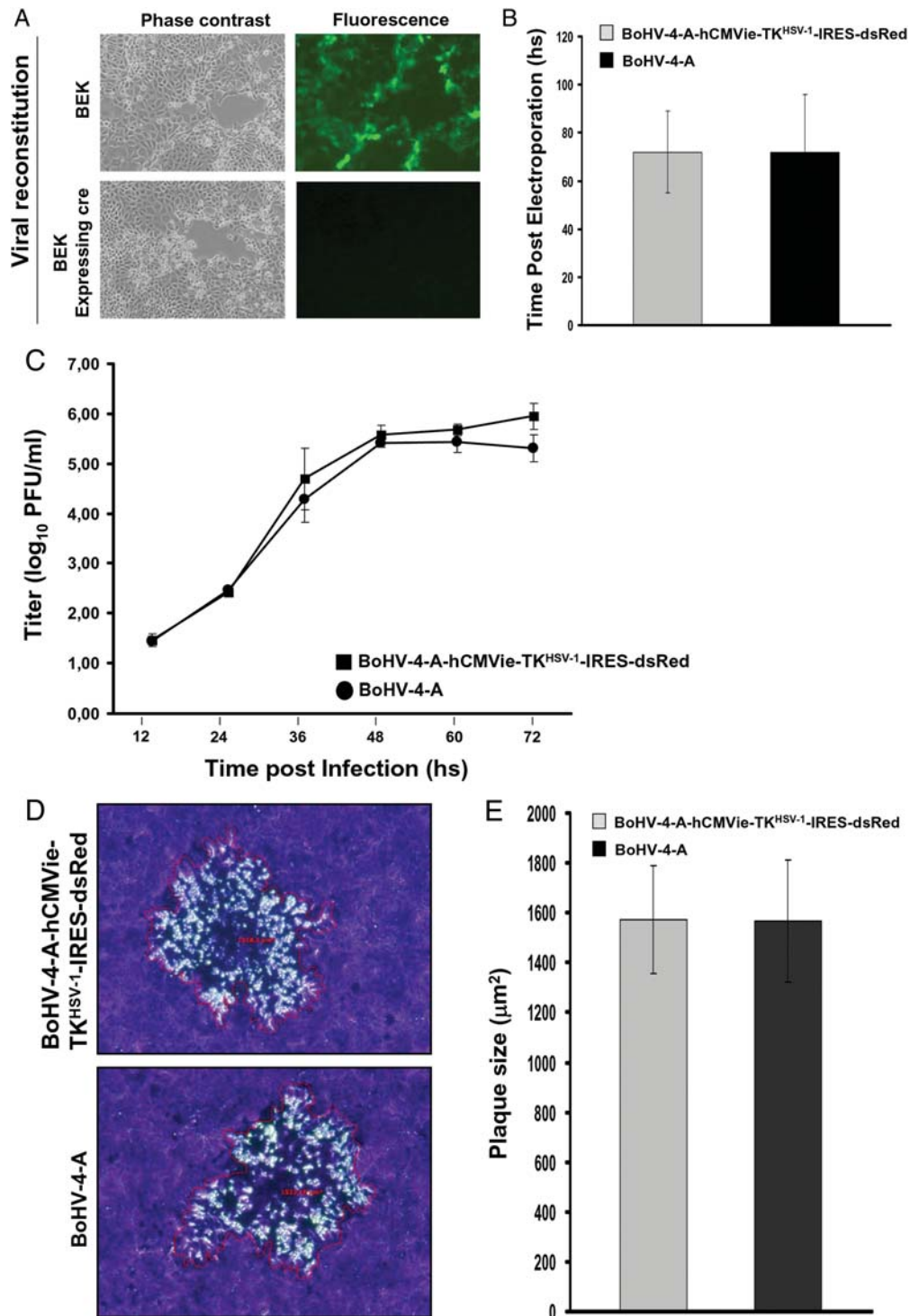


Fig. 2. A, Representative images (phase contrast or fluorescence, 10X) of BoHV-4-A-hCMVie-TK<sup>HSV-1</sup>-IRES-dsRed virus reconstitution following pBAC-BoHV-4-A-hCMVie-TK<sup>HSV-1</sup>-IRES-dsRed-pA electroporation into BEK or BEK expressing cre recombinase. B, Time after electroporation (hours) employed by pBAC-BoHV-4-A-hCMVie-TK<sup>HSV-1</sup>-IRES-dsRed-pA and pBAC-BoHV-4 to get viral reconstitution and plaque formation, following electroporation into BEK expressing cre cells (The data presented are the means  $\pm$  standard errors of 3 electroporation for each BAC). C, Replication kinetics of BoHV-4-A-hCMVie-TK<sup>HSV-1</sup>-IRES-dsRed compared with BoHV-4-A. The data presented are the means  $\pm$  standard errors of triplicate measurements ( $P > .05$  for all time points as measured by Student's *t* test). D, Representative images (10X) of plaque morphology and relative plaque size of BoHV-4-A-hCMVie-TK<sup>HSV-1</sup>-IRES-dsRed and BoHV-4-A on Vero cells. E, The plaque sizes ( $\mu\text{m}^2$ ) were measured using the Axio-Vision40-V4.6.3.0 (Carl Zeiss, Imaging Solution, <http://www.zeiss.de/C12567BE0045ACF1/ContentsFrame/668C9FDCBB18C6E2412568C10045A72E>) software program. Bars represent means  $\pm$  standard errors of 50 plaques for each virus;  $P > .05$ .

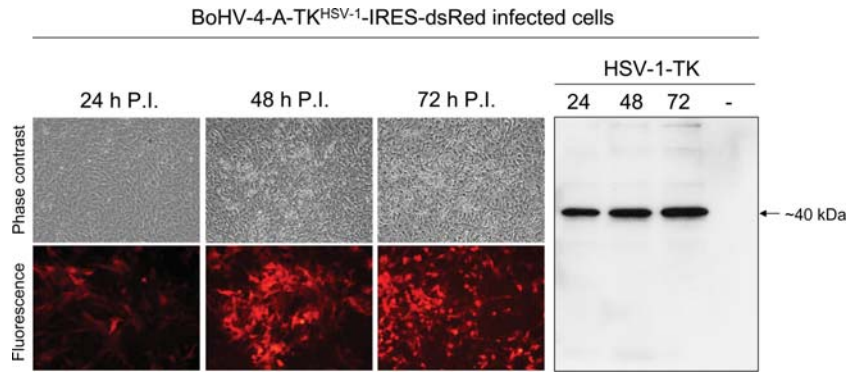


Fig. 3. Representative BoHV-4-A-TK<sup>HSV-1</sup>-IRES-dsRed infected cell line (10X) at different time post infection (24, 48, and 72 h) expressing red fluorescent protein (fluorescence and phase contrast microscope images) and HSV-1-TK (Western immunoblotting). Negative control was made with a cell extract coming from uninfected cells (-).

impairment using a clinical assessment scale.<sup>18</sup> The survival rate was measured by Kaplan-Meier curves and log-rank test (Fig. 7). Brain tumor of treated or untreated animals were histologically examined at the end of each experiment for tumor regression (Supplementary File 2).

In mice, the survival comparison reported in Fig. 7B shows a significant increase in survival in the groups treated with BoHV-4-A-hCMVie-TK<sup>HSV-1</sup>-IRES-dsRed ( $n = 12$ ) or with BoHV-4-A-hCMVie-TK<sup>HSV-1</sup>-IRES-dsRed + GCV ( $n = 12$ ; log-rank test,  $\chi_{1,3} = 25,06$ ,  $P < .001$ ), compared with PBS- or GCV-treated groups. However, the difference of survival between the BoHV-4-A-hCMVie-TK<sup>HSV-1</sup>-IRES-dsRed and BoHV-4-A-hCMVie-TK<sup>HSV-1</sup>-IRES-dsRed + GCV groups was not statistically significant.

In rats, the increase in survival (Fig. 7C) shown by the BoHV-4-A-hCMVie-TK<sup>HSV-1</sup>-IRES-dsRed + GCV group was statistically significant if compared with each of the other 3 groups ( $n = 8$ ; log-rank test,  $\chi_{1,3} = 14,96$ ,  $P < .005$ ). At present, one animal is still alive at 230 days posttreatment.

## Discussion

The complexity and plasticity of tumors, such as gliomas, dictates that combination therapies should be used to generate effective and durable responses in the patient with cancer. Armed therapeutic viruses that couple lytic replication of the virus with the capability to deliver therapeutic factors (armed therapeutic viruses) are an obvious evolution of oncolytic virus-based therapy. This approach takes advantage of the viruses' ability to selectively replicate and spread into the tumor mass and to safely and efficiently deliver therapeutic genes to target tissues, where the therapeutic gene products can accumulate to levels that induce maximal tumor cell death. Therefore, the choice of the appropriate gene(s) to enable the oncolytic virus to arrest or eradicate highly plastic, rapidly evolving tumor is a crucial issue.<sup>25</sup>

During lytic infection, many herpesviruses induce a virus-specific deoxy-pyrimidine kinase (TK), an

enzyme involved in the salvage pathway of pyrimidine biosynthesis.<sup>26</sup> It has been shown that some defective (TK<sup>-</sup>) herpesvirus mutants have some replication deficiencies in vitro and restricted growth in vivo when compared with the wild-type virus, particularly with respect to their inability to reactivate from the latent state.<sup>27</sup> BoHV-4, like many other herpesviruses, has a TK gene, and the translated product of the BoHV-4 TK ORF is a 445 amino acid protein of predicted  $M_r$  50862.<sup>28</sup> The percentages of amino acid identity and similarity observed between BoHV-4 and several herpesvirus TKs are relatively low, because TK is not a conserved protein among herpesviruses.<sup>29</sup> However, the percentage of homology between BoHV-4 and HVS TK has been shown to be higher than those between EBV TK and BoHV-4 or HVS TK.<sup>28</sup> This is in agreement with the strong colinearity between the HVS and BoHV-4 genome and a similar TK enzyme activity.<sup>23</sup> BoHV-4 induces a novel TK activity in the cytosol fraction of the BoHV-4-infected TK<sup>-</sup> rabbit skin cell mutants, and this activity is similar to that observed for HVS TK,<sup>23</sup> where a lack of effect toward nucleoside analogs, such as GCV, was observed.<sup>23</sup> Starting from this specific data, it was decided to substitute BoHV-4 TK with HSV-1 TK, which phosphorylates GCV. The BoHV-4 TK gene has been disrupted in BoHV-4 by the insertion of foreign sequences without interfering with viral replication in vitro.<sup>16</sup> Furthermore, the BoHV-4 TK genomic region is highly conserved among BoHV-4 isolates,<sup>28</sup> ensuring the stability of the genomic locus for the insertion of foreign expression cassettes. Therefore, the BoHV-4 TK gene was chosen as a target site for the insertion of an hCMVie-TK<sup>HSV-1</sup>-IRES-dsRed-pA expression cassette into the BoHV-4-A genome, cloned as BAC. The BAC recombinering system approach<sup>30</sup> modified by the introduction of a kanamycin selection step was used for this purpose, as previously described.<sup>31</sup> Thus, a recombinant BoHV-4 expressing HSV-1 TK and RFP in a bicistronic fashion was successfully obtained.

BoHV-4 has a relatively slow kinetic of TK enzyme induction when compared with HSV-1; cytosolic extracts from BoHV-4-infected TK<sup>-</sup> rabbit skin cell



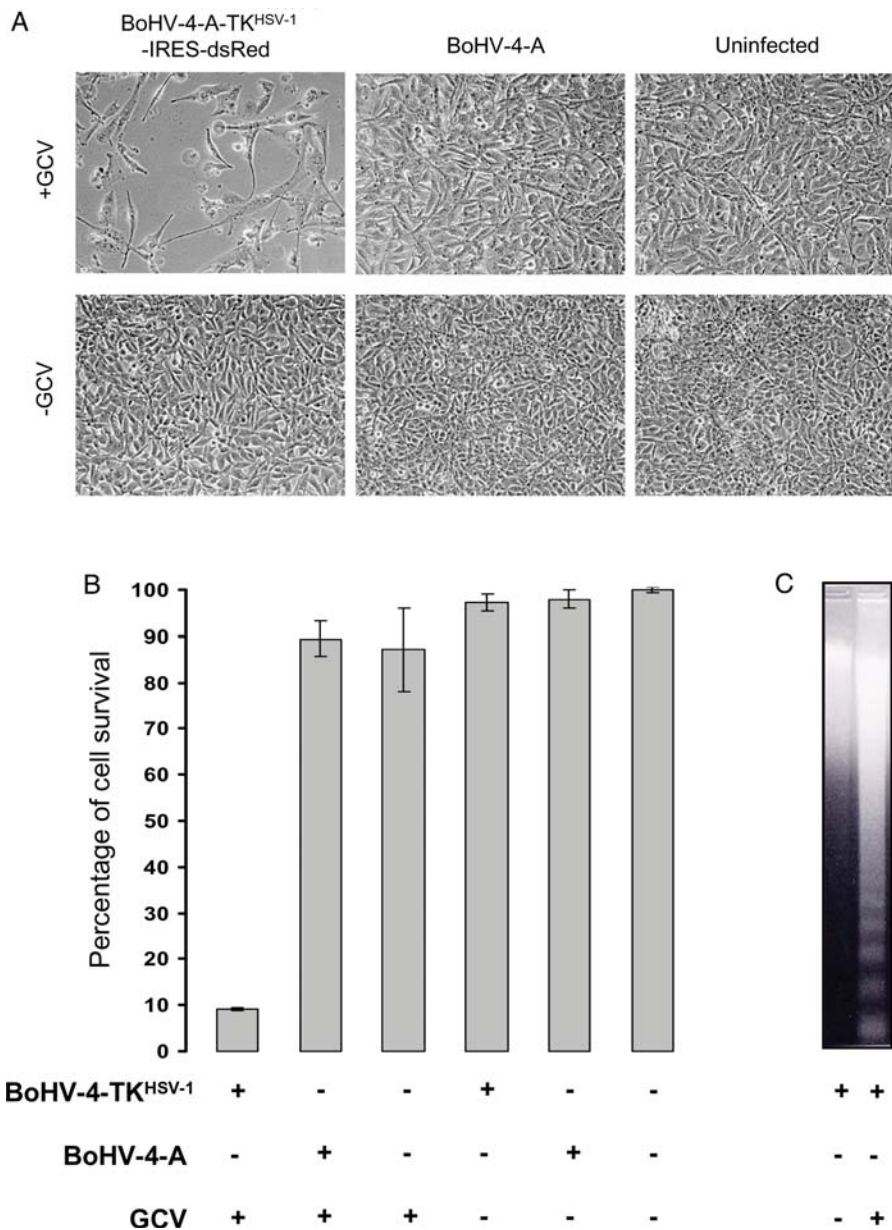


Fig. 4. A, Phase contrast microscope images of RD-4 cells (10X) infected with BoHV-4-A-TK<sup>HSV-1</sup>-IRES-dsRed (BoHV-4<sup>TK<sup>HSV-1</sup></sup>) or BoHV-4-A and treated (GCV+) or untreated (GCV-) with GCV. B, Infection and treatment quantified by MTT assay. (The data presented are the means  $\pm$  standard errors of three different experiments). C, Representative images of apoptotic cell death detected by DNA laddering in cells infected with BoHV-4-A-TK<sup>HSV-1</sup>-IRES-dsRed (BoHV-4-TK<sup>HSV-1</sup>) and treated with GCV but not with the other combinations of infection/treatment.

mutants catalyze the phosphorylation of [H<sup>3</sup>]dThd to dTMP, dTDP, and dTTP at 16 h pi and sharply increase to a maximum at  $\sim$ 24 h postinfection, whereas HSV-1TK activity can be detected as early as 2.5 h postinfection and reach the maximum by 5–7 h postinfection.<sup>23</sup> Because these data correlate with the slow replication cycle of BoHV-4 and the fast replication cycle of HSV-1, it was of interest to investigate the replication kinetics of BoHV-4 delivering HSV-1 TK. Of surprise, BoHV-4-A-TK<sup>HSV-1</sup>-IRES-dsRed had an identical replication kinetic of BoHV-4-A; therefore, BoHV-4

replication does not seem to be correlated with TK activity.

Expression of HSV-1 TK to activate the HSV-1 TK-selective aciclovir-derived prodrug 9-([2-hydroxy-1-(hydroxymethyl)ethoxy]methyl) guanine (GCV) was used for the first proof-of-principle of suicide gene therapy.<sup>32</sup> The HSV-1 TK GCV combination and variations thereof remain the most widely used systems in both clinical and experimental gene-directed enzyme prodrug therapy applications. HSV-1 TK has a different catalytic specificity to mammalian TKs, exhibiting

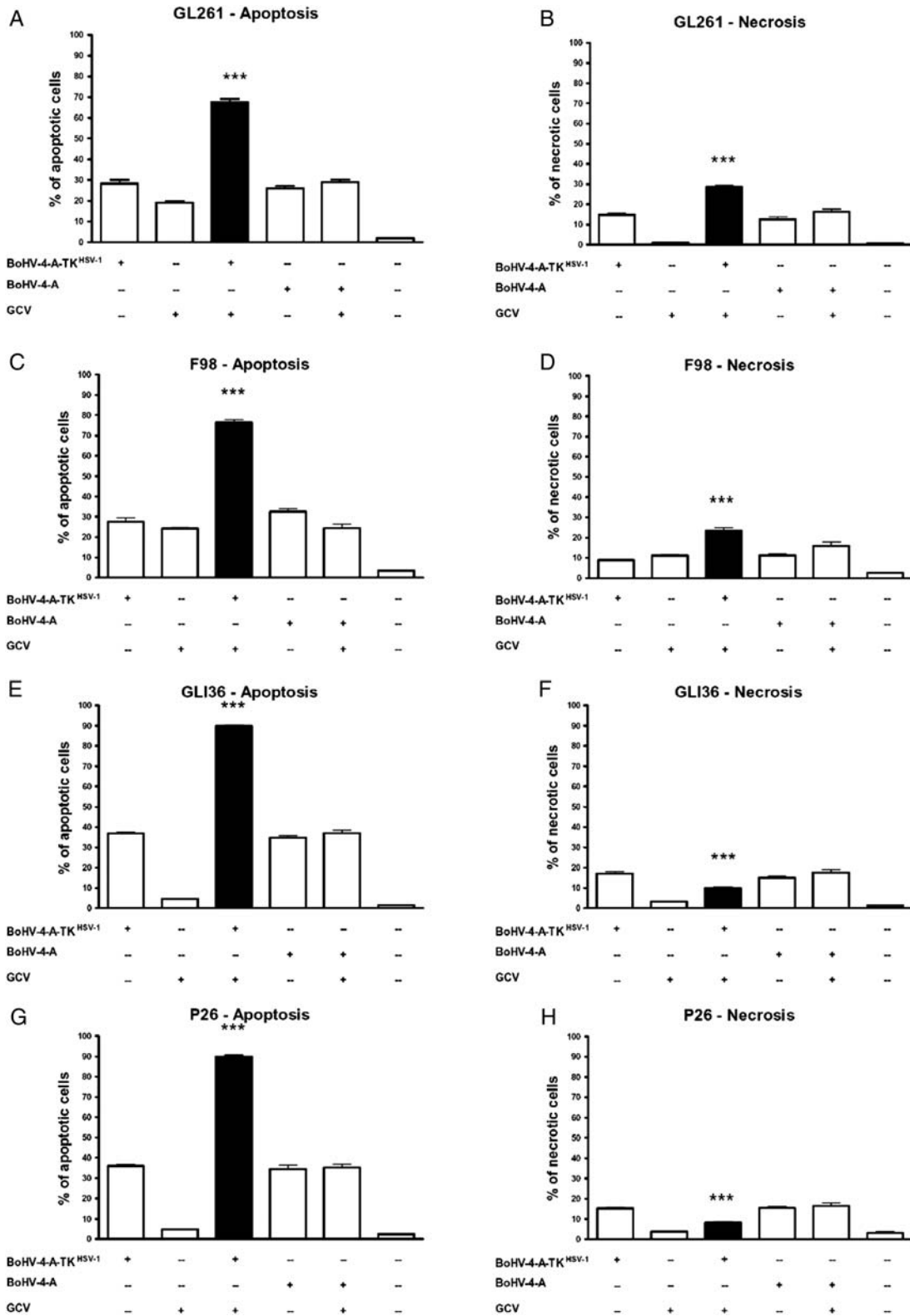


Fig. 5. Percentage (mean  $\pm$  standard error of the mean) of apoptosis (A, C, E, and G) and necrosis (B, D, F, and H) induced by different BoHV-4 based treatments in different glioma cells: GL261 (A and B), F98 (C and D), GLI36 (E and F) and P26 (G and H). The black bar represents the treatment with BoHV-4-A-TK<sup>HSV-1</sup>-IRES-dsRed (BoHV-4-TK<sup>HSV-1</sup>) + GCV and it has been compared to each of the other conditions with *t* test. In A, B, C, D, E, and G the induced cell death is higher in BoHV-4-TK<sup>HSV-1</sup> + GCV than in each of the other treatment. In F and H the induced necrosis was significantly lower if compared to the other BoHV-4 groups and significantly higher if compared to the GCV and control groups (\*\**t* test,  $P < .001$ . The data presented are the means  $\pm$  standard errors of 3 different experiments).

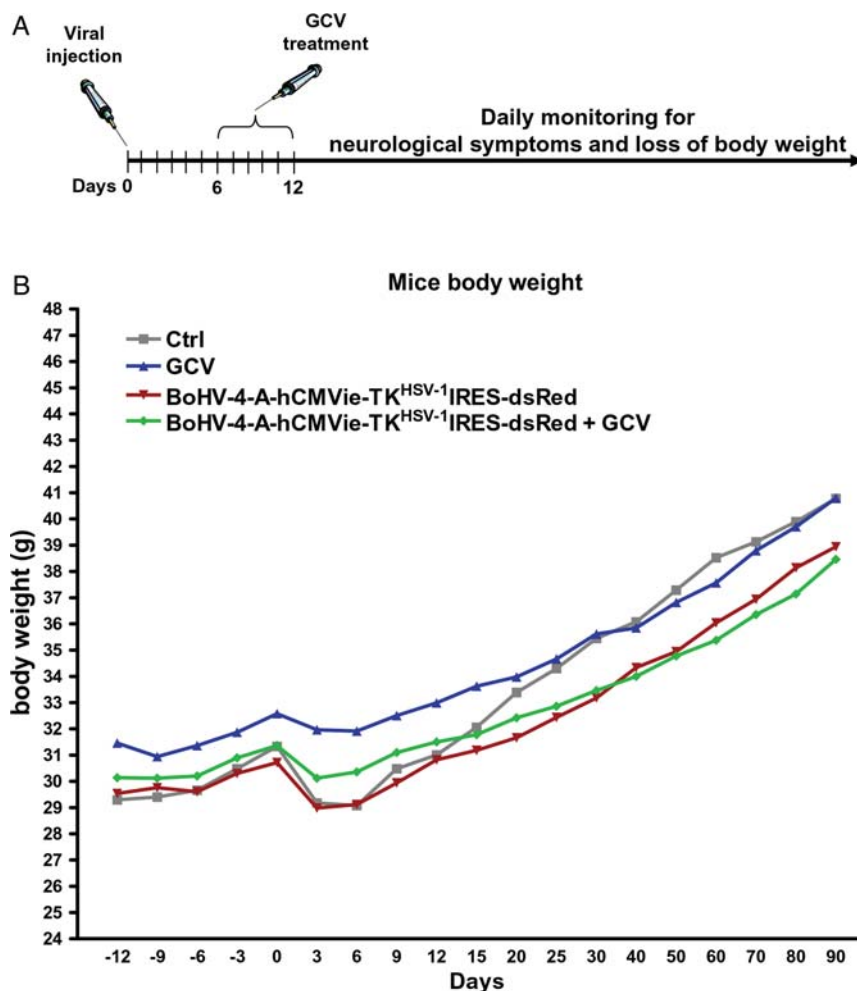


Fig. 6. A, Diagram exemplifying the experimental strategy used. B, Body weight gain in healthy mice treated with BoHV-4-A-TK<sup>HSV-1</sup>-IRES-dsRed and GCV, BoHV-4-A-TK<sup>HSV-1</sup>-IRES-dsRed, GCV or PBS. The curves were analyzed with one way ANOVA and no differences were found.

~1000-fold greater efficiency in monophosphorylating GCV-MP),<sup>33</sup> which is the rate-limiting step in the conversion of GCV to its cytotoxic metabolites. This property provided the basis for both the development of GCV as an anti-herpetic drug and the application of HSV-1 TK as a suicide gene for cancer gene therapy. Following the monophosphorylation of GCV to monophosphorylating GCV by HSV-1 TK, monophosphorylating GCV is subsequently further phosphorylated to its diphosphate and triphosphate forms by endogenous guanylate kinase and several other enzymes, such as phosphoglycerate kinase.<sup>34</sup> Triphosphate GCV, the most active of a number of toxic metabolites of GCV, exerts its cytotoxic effects intracellularly both by inhibiting cellular DNA polymerases<sup>35</sup> and by competing with deoxyguanosine triphosphate for incorporation into nascent DNA molecules during cell division,<sup>34</sup> leading inevitably to single-strand breaks and, ultimately, to death of the affected cell.<sup>34</sup>

The precise mechanism of HSV-1 TK GCV-mediated cell death is still not completely understood. Although, in general, it seems that apoptosis plays the major role

in this process, nonapoptotic mechanisms may also be involved, often seemingly dependent on the specific cell type to which the system is applied.<sup>34</sup> In fact, when BoHV-4-A-TK<sup>HSV-1</sup>-IRES-dsRed was used to infect RD-4 cells, they died by apoptosis following treatment with GCV, in contrast to BoHV-4-A-TK<sup>HSV-1</sup>-IRES-dsRed untreated with GCV or BoHV-4-A-infected RD-4 cells treated with GCV, which survived. Thus, this confirmed the suicide behavior of BoHV-4 in the presence of GCV and only when provided with HSV-1 TK ORF (BoHV-4-A-TK<sup>HSV-1</sup>-IRES-dsRed). These data were then corroborated by the strong increase in apoptosis with respect to necrosis when GL261, F98, GLI36, and P26 cell lines were infected and treated with BoHV-4-A-TK<sup>HSV-1</sup>-IRES-dsRed/GCV.<sup>36–38</sup>

BoHV-4 injection within the lateral ventricle of mouse and rat brain established the transduction of glial fibrillary acidic protein positive (GFAP<sup>+</sup>) cells along the rostral migratory stream in absence of viral replication.<sup>18,19</sup> With this in mind, it was of concern that these GFAP<sup>+</sup> cells could be depleted after BoHV-4-A-TK<sup>HSV-1</sup>-IRES-dsRed/GCV treatment, resulting in an

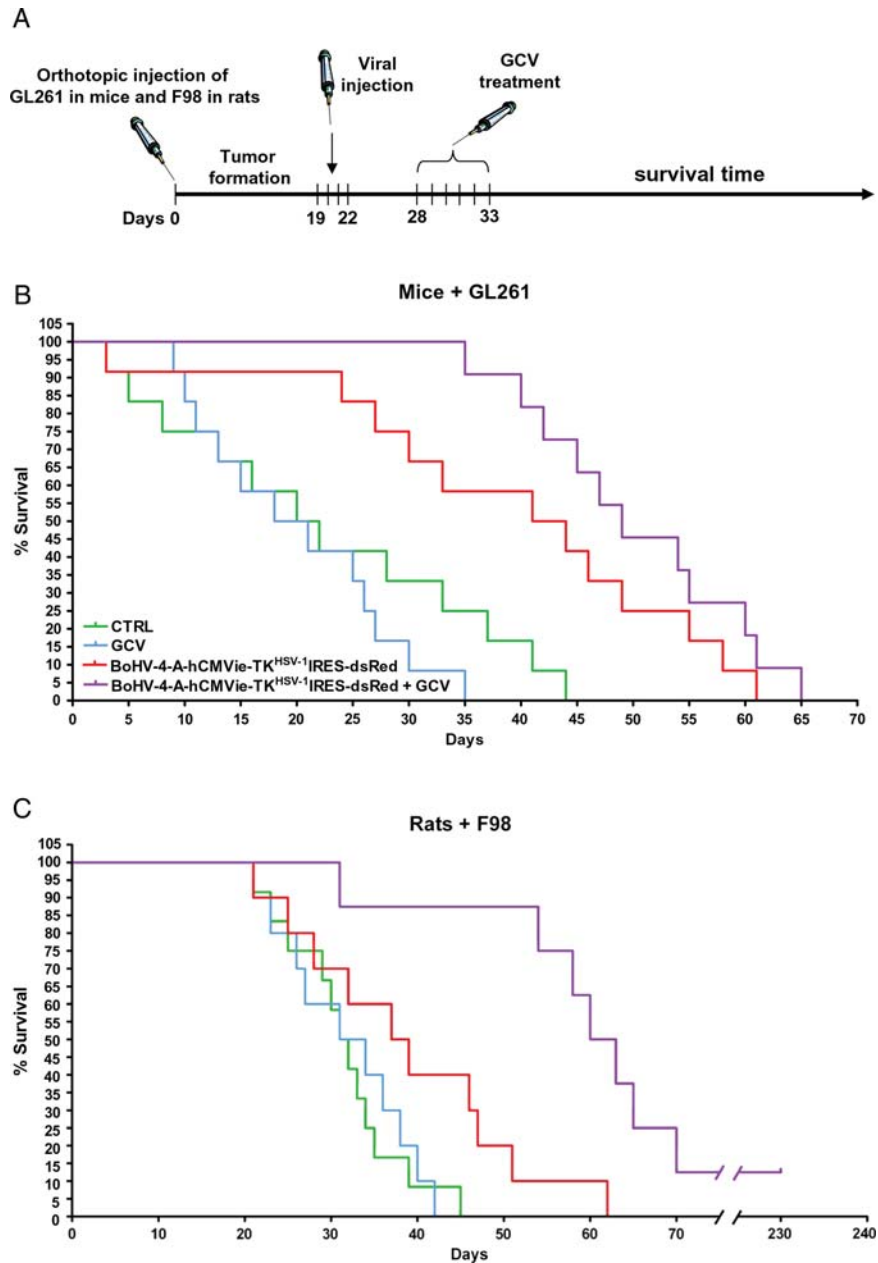


Fig. 7. A, Diagram exemplifying the experimental strategy employed. B, Kaplan-Meier survival curves of GL261 tumor-bearing C57BL/6 mice ( $n = 48$ ). The curves show a significant difference (log-rank test,  $\chi_{1,3} = 25.06$ ,  $P < .001$ ) between the BoHV-4-A-TK<sup>HSV-1</sup>-IRES-dsRed based groups (2 groups of 12 subjects) and the other groups (2 groups of 12 subjects). C, Kaplan-Meier survival curves of F98 tumor-bearing Fisher rats ( $n = 40$ ). The BoHV-4-A-TK<sup>HSV-1</sup>-IRES-dsRed + GCV group ( $n = 8$ ) shows a statistically significant increase of survival if compared with each of the other groups (log-rank test,  $\chi_{1,3} = 14.96$ ,  $P < .005$ ).

alteration of brain function. Therefore, healthy mice were BoHV-4-A-TK<sup>HSV-1</sup>-IRES-dsRed/GCV treated; neither sign of neurological symptoms nor progressive loss of body weight were observed, suggesting that BoHV-4-A-TK<sup>HSV-1</sup>-IRES-dsRed/GCV treatment was definitely not neurotoxic in vivo. The BoHV-4-A-TK<sup>HSV-1</sup>-IRES-dsRed/GCV therapeutic approach was strongly encouraging when applied in vitro and nonneurotoxic in healthy mice in vivo. Therefore, we tested BoHV-4-A-TK<sup>HSV-1</sup>-IRES-dsRed/GCV treatment on gliomas in vivo in an animal model that closely mimics

human disease. A clear distinction should be made between glioma-genesis in genetically engineered rodents (mainly transgenic mice over-expressing oncogenes or in which a tumor suppressor gene has been deleted) and engrafted tumor models (primary tumor cells or tumor cell lines that have been implanted into mouse and rat brain). The former models more closely resemble human gliomas, but they have poor reproducibility, low tumor penetrance, and slow growth. On the other hand, the engrafted models have good reproducibility, high grade of tumor penetrance, and relatively fast

growth. For these reasons and as a good compromise, the mouse and rat immunocompetent orthotopic engrafted syngenic models based on GL261<sup>39</sup> and F98<sup>40</sup> glioma cell lines were adopted. Gliomas were successfully generated in mice and rats with good efficiency. BoHV-4-A-TK<sup>HSV-1</sup>-IRES-dsRed/GCV treatment resulted in a longer survival time with respect to the control groups. The F98 glioma in Fisher rats, similarly to GBMs in human, is composed of a mixed population of spindle-shaped cells over-expressing PDGF $\beta$ , Ras, EGFR, Cyclin D1, and Cyclin D2. Furthermore, it simulates human GBM characteristics in a number of relevant ways, such as its highly invasive pattern of growth, low immunogenicity, and resistance to a number of therapeutic modalities, including systemic chemotherapy<sup>41</sup> and photon-irradiation.<sup>42</sup>

In previous studies, we reported the capacity of BoHV-4 to infect and replicate in glioma cell lines and glioblastoma primary cultures in vitro and the ability of BoHV-4 to selectively infect gliomas induced in the rat brain in vivo.<sup>19,20</sup> In this article, we extend our findings to suggest a possible use of BoHV-4 as a therapeutic vector in the treatment of glioma. The large number of available studies on glioma therapy underlines the need to extensively investigate many models before moving to clinical trials.<sup>43,44</sup> In particular, the results from gene therapy present many difficulties in the move from the laboratory bench to the clinical setting.<sup>45,46</sup> All of the gene therapy-based research points to the safety of the vectors used.<sup>47,48</sup> Here, we demonstrated the safety of the BoHV-4 delivering HSV-1 TK also in association with GCV and the efficiency of the treatment

both in vitro (apoptosis induction) and in vivo (survival). Further studies will involve a more in-depth investigation of the relationship between glioma cells and our vector, to better understand the infection mechanism. In conclusion, all of the presented data support BoHV-4 delivering HSV-1 TK associated with GCV as a possible oncolytic treatment for gliomas.

## Supplementary Material

Supplementary material is available at *Neuro-Oncology Journal* online (<http://neuro-oncology.oxfordjournals.org/>).

## Acknowledgment

We thank the Italian Ministry of University and Scientific Research for financial support; Professor Cavaggioni Andrea for his intellectual support; and Dr. Scott W. Wong and Dr. Laura Kramer for the English language correction.

*Conflict of interest statement.* None declared.

## Funding

Italian Ministry of University and Scientific Research (Italian National Grant MIUR, PRIN 2008).

## References

- Kleihues P, Sobin LH. World Health Organization classification of tumors. *Cancer*. 2000;88(12):2887.
- Burton EC, Prados MD. Malignant gliomas. *Current Treatment Options in Oncology*. 2000;1(5):459–468.
- Ohgaki H, Kleihues P. Population-based studies on incidence, survival rates, and genetic alterations in astrocytic and oligodendroglial gliomas. *Journal of Neuropathology and Experimental Neurology*. 2005;64(6):479–489.
- Ohgaki H, Kleihues P. Epidemiology and etiology of gliomas. *Acta Neuropathologica*. 2005;109(1):93–108.
- Cassady KA, Parker JN. Herpesvirus vectors for therapy of brain tumors. *The Open Virology Journal*. 2010;4:103–108.
- Thiry E, Dubuisson J, Bublot M, Van Bressemer MF, Pastoret PP. The biology of bovine herpesvirus-4 infection of cattle. *Dtsch Tierarztl Wochenschr*. 1990;97(2):72–77.
- Bartha A, Juhasz M, Liebermann H. Isolation of a bovine herpesvirus from calves with respiratory disease and keratoconjunctivitis. A preliminary report. *Acta Veterinaria Academiae Scientiarum Hungaricae*. 1966;16(3):357–358.
- Mohanty SB, Hammond RC, Lillie MG. A new bovine herpesvirus and its effect on experimentally infected calves. Brief report. *Archiv fur die gesamte Virusforschung*. 1971;33(3):394–395.
- Dubuisson J, Thiry E, Thalasso F, Bublot M, Pastoret PP. Biological and biochemical comparison of bovid herpesvirus-4 strains. *Veterinary Microbiology*. 1988;16(4):339–349.
- Osorio FA, Rock DL, Reed DE. Studies on the pathogenesis of a bovine cytomegalo-like virus in an experimental host. *The Journal of General Virology*. 1985;66(Pt 9):1941–1951.
- Storz J, Ehlers B, Todd WJ, Ludwig H. Bovine cytomegaloviruses: identification and differential properties. *The Journal of General Virology*. 1984;65(Pt 4):697–706.
- Zimmermann W, Broll H, Ehlers B, Buhk HJ, Rosenthal A, Goltz M. Genome sequence of bovine herpesvirus 4, a bovine Rhadinovirus, and identification of an origin of DNA replication. *Journal of Virology*. 2001;75(3):1186–1194.
- Peterson RB, Goyal SM. Propagation and quantitation of animal herpesviruses in eight cell culture systems. *Comparative Immunology, Microbiology and Infectious Diseases*. 1988;11(2):93–98.
- Gillet L, Minner F, Detry B, et al. Investigation of the susceptibility of human cell lines to bovine herpesvirus 4 infection: demonstration that human cells can support a nonpermissive persistent infection which protects them against tumor necrosis factor alpha-induced apoptosis. *Journal of Virology*. 2004;78(5):2336–2347.
- Gillet L, Dewals B, Farnir F, de Leval L, Vanderplasschen A. Bovine herpesvirus 4 induces apoptosis of human carcinoma cell lines in vitro and in vivo. *Cancer Research*. 2005;65(20):9463–9472.
- Donofrio G, Cavirani S, Simone T, van Santen VL. Potential of bovine herpesvirus 4 as a gene delivery vector. *Journal of Virological Methods*. 2002;101(1–2):49–61.

17. Donofrio G, Sartori C, Franceschi V, et al. Double immunization strategy with a BoHV-4-vectorized secreted chimeric peptide BVDV-E2/BoHV-1-gD. *Vaccine*. 2008;26(48):6031–6042.
18. Donofrio G, Cavaggioni A, Bondi M, Cavirani S, Flammini CF, Mucignat-Caretta C. Outcome of bovine herpesvirus 4 infection following direct viral injection in the lateral ventricle of the mouse brain. *Microbes Infect*. 2006;8(3):898–904.
19. Redaelli M, Cavaggioni A, Mucignat-Caretta C, Cavirani S, Caretta A, Donofrio G. Transduction of the rat brain by Bovine Herpesvirus 4. *Genet Vaccines Ther*. 2008;6:6.
20. Redaelli M, Mucignat-Caretta C, Cavaggioni A, et al. Bovine herpesvirus 4 based vector as a potential oncolytic-virus for treatment of glioma. *Virology Journal*. 2010;7:298.
21. Donofrio G, Franceschi V, Capocéfalo A, et al. Cellular targeting of engineered heterologous antigens is a determinant factor for bovine herpesvirus 4-based vaccine vector development. *Clin Vaccine Immunol*. 2009;16(11):1675–1686.
22. Mucignat-Caretta C, Cavaggioni A, Redaelli M, Malatesta M, Zancanaro C, Caretta A. Selective distribution of protein kinase A regulatory subunit RII{alpha} in rodent gliomas. *Neuro-oncology*. 2008;10(6):958–967.
23. Kit S, Kit M, Ichimura H, Crandell R, McConnell S. Induction of thymidine kinase activity by viruses with group B DNA genomes: bovine cytomegalovirus (bovine herpesvirus 4). *Virus Research*. 1986;4(2):197–212.
24. Donofrio G, Cavirani S, van Santen VL. Establishment of a cell line persistently infected with bovine herpesvirus-4 by use of a recombinant virus. *The Journal of General Virology*. 2000;81(Pt 7):1807–1814.
25. Hermiston TW, Kuhn I. Armed therapeutic viruses: strategies and challenges to arming oncolytic viruses with therapeutic genes. *Cancer Gene Therapy*. 2002;9(12):1022–1035.
26. Kit S. Thymidine kinase. *Microbiological Sciences*. 1985;2(12):369–375.
27. Efstathiou S, Kemp S, Darby G, Minson AC. The role of herpes simplex virus type 1 thymidine kinase in pathogenesis. *The Journal of General Virology*. 1989;70(Pt 4):869–879.
28. Lomonte P, Bublot M, Pastoret PP, Thiry E. Location and characterization of the bovine herpesvirus type 4 thymidine kinase gene; comparison with thymidine kinase genes of other herpesviruses. *Archives of Virology*. 1992;127(1–4):327–337.
29. Honess RW, Craxton MA, Williams L, Gompels UA. A comparative analysis of the sequence of the thymidine kinase gene of a gammaherpesvirus, herpesvirus saimiri. *The Journal of General Virology*. 1989;70(Pt 11):3003–3013.
30. Warming S, Costantino N, Court DL, Jenkins NA, Copeland NG. Simple and highly efficient BAC recombineering using galK selection. *Nucleic Acids Res*. 2005;33(4):e36.
31. Donofrio G, Sartori C, Ravanetti L, et al. Establishment of a bovine herpesvirus 4 based vector expressing a secreted form of the bovine viral diarrhoea virus structural glycoprotein E2 for immunization purposes. *BMC Biotechnol*. 2007;7:68.
32. Moolten FL. Tumor chemosensitivity conferred by inserted herpes thymidine kinase genes: paradigm for a prospective cancer control strategy. *Cancer Research*. 1986;46(10):5276–5281.
33. Elion GB, Furman PA, Fyfe JA, de Miranda P, Beauchamp L, Schaeffer HJ. Selectivity of action of an antiherpetic agent, 9-(2-hydroxyethoxymethyl) guanine. *Proceedings of the National Academy of Sciences of the United States of America*. 1977;74(12):5716–5720.
34. Fillat C, Carrio M, Cascante A, Sangro B. Suicide gene therapy mediated by the Herpes Simplex virus thymidine kinase gene/Ganciclovir system: fifteen years of application. *Current Gene Therapy*. 2003;3(1):13–26.
35. Ilsley DD, Lee SH, Miller WH, Kuchta RD. Acyclic guanosine analogs inhibit DNA polymerases alpha, delta, and epsilon with very different potencies and have unique mechanisms of action. *Biochemistry*. 1995;34(8):2504–2510.
36. Aghi M, Chou TC, Suling K, Breakefield XO, Chiocca EA. Multimodal cancer treatment mediated by a replicating oncolytic virus that delivers the oxazaphosphorine/rat cytochrome P450 2B1 and ganciclovir/herpes simplex virus thymidine kinase gene therapies. *Cancer Research*. 1999;59(16):3861–3865.
37. Boviatsis EJ, Park JS, Sena-Esteves M, et al. Long-term survival of rats harboring brain neoplasms treated with ganciclovir and a herpes simplex virus vector that retains an intact thymidine kinase gene. *Cancer Research*. 1994;54(22):5745–5751.
38. Carroll NM, Chase M, Chiocca EA, Tanabe KK. The effect of ganciclovir on herpes simplex virus-mediated oncolysis. *The Journal of Surgical Research*. 1997;69(2):413–417.
39. Szatmari T, Lumniczky K, Desaknai S, et al. Detailed characterization of the mouse glioma 261 tumor model for experimental glioblastoma therapy. *Cancer Science*. 2006;97(6):546–553.
40. Mathieu D, Lecomte R, Tsanaclis AM, Larouche A, Fortin D. Standardization and detailed characterization of the syngeneic Fischer/F98 glioma model. *The Canadian Journal of Neurological Sciences*. 2007;34(3):296–306.
41. von Eckardstein KL, Patt S, Kratzel C, Kiwit JC, Reszka R. Local chemotherapy of F98 rat glioblastoma with paclitaxel and carboplatin embedded in liquid crystalline cubic phases. *Journal of Neuro-oncology*. 2005;72(3):209–215.
42. Barth RF. Rat brain tumor models in experimental neuro-oncology: the 9L, C6, T9, F98, RG2 (D74), RT-2 and CNS-1 gliomas. *Journal of Neuro-oncology*. 1998;36(1):91–102.
43. Fueyo J, Gomez-Manzano C, Yung WK. Advances in translational research in neuro-oncology. *Archives of Neurology*. 2011;68(3):303–308.
44. Maes W, Van Gool SW. Experimental immunotherapy for malignant glioma: lessons from two decades of research in the GL261 model. *Cancer Immunol Immunother*. 2011;60(2):153–160.
45. Gabhann FM, Annex BH, Popel AS. Gene therapy from the perspective of systems biology. *Current Opinion in Molecular Therapeutics*. 2010;12(5):570–577.
46. Hughes SA, Achanta P, Ho AL, Duenas VJ, Quinones-Hinojosa A. Biological horizons for targeting brain malignancy. *Advances in Experimental Medicine and Biology*. 2011;671:93–104.
47. Colombo F, Barzon L, Franchin E, et al. Combined HSV-TK/IL-2 gene therapy in patients with recurrent glioblastoma multiforme: biological and clinical results. *Cancer Gene Therapy*. 2005;12(10):835–848.
48. Castro MG, Candolfi M, Kroeger K, et al. Gene therapy and targeted toxins for glioma. *Current Gene Therapy*. 2011;11(3):155–180.